Effect of Auger recombination and leakage on the droop in InGaN/GaN quantum well LEDs

Friedhard Römer* and Bernd Witzigmann

Computational Electronics and Photonics Group, Dept. of Electrical Engineering, University of Kassel, 34121 Kassel, Germany

*froemer@uni-kassel.de

Abstract

We investigate the effect of the epitaxial structure and the acceptor doping profile on the efficiency droop in InGaN/GaN LEDs by the physics based simulation of experimental internal quantum efficiency (IQE) characteristics. The device geometry is an integral part of our simulation approach. We demonstrate that even for single quantum well LEDs the droop depends critically on the acceptor doping profile. The Auger recombination was found to increase stronger than with the third power of the carrier density and has been found to dominate the droop in the roll over zone of the IQE. The fitted Auger coefficients are in the range of the values predicted by atomistic simulations.

References

[1] A. Laubsch, M. Sabathil, J. Baur, M. Peter, and B. Hahn, "High-Power and High-Efficiency InGaN-Based Light Emitters," IEEE Trans. Electron Devices **57**, 79–87 (2010).

[2] J. Piprek, "Efficiency droop in nitride-based light-emitting diodes," Phys. Status Solidi A **207**, 2217–2225 (2010).

[3] J. Cho, E. F. Schubert, and J. K. Kim, "Efficiency droop in light-emitting diodes: Challenges and countermeasures," Laser Photonics Rev. **7**, 408–421 (2013).

[4] T. T. Mnatsakanov, M. E. Levinshtein, L. I. Pomortseva, S. N. Yurkov, G. S. Simin, and M. Asif Khan, "Carrier mobility model for GaN," Solid-State Electron. **47**, 111–115 (2003).

[5] M. Deppner, F. Römer, and B. Witzigmann, "Auger carrier leakage in III-nitride quantum-well light emitting diodes," Phys. Status Solidi RRL **6**, 418–420 (2012).

[6] J. Iveland, L. Martinelli, J. Peretti, J. S. Speck, and C. Weisbuch, "Direct Measurement of Auger Electrons Emitted from a Semiconductor Light-Emitting Diode under Electrical Injection: Identification of the Dominant Mechanism for Efficiency Droop," Phys. Rev. Lett. **110**, 177406 (2013).

[7] M. Binder, A. Nirschl, R. Zeisel, T. Hager, H.-J. Lugauer, M. Sabathil, D. Bougeard, J. Wagner, and B. Galler, "Identification of nnp and npp Auger recombination as significant contributor to the efficiency droop in (GaIn)N quantum wells by visualization of hot carriers in photoluminescence," Appl. Phys. Lett. **103**, 071108 (2013).

[8] E. Kioupakis, P. Rinke, K. T. Delaney, and C. G. Van de Walle, "Indirect Auger recombination as a cause of efficiency droop in nitride light-emitting diodes," Appl. Phys. Lett. **98**, 161107 (2011).

[9] B. Witzigmann, R. G. Veprek, S. Steiger, and J. Kupec, "Comprehensive modeling of optoelectronic nanostructures," J. Comput. Electron. **8**, 389–397 (2009).

[10] S. Steiger, R. G. Veprek, and B. Witzigmann, "Unified simulation of transport and luminescence in optoelectronic nanostructures," J. Comput. Electron. **7**, 509–520 (2008).

[11] F. Römer, M. Deppner, C. Range, and B. Witzigmann, "Auger recombination and leakage in InGaN/GaN quantum well LEDs," Proc. SPIE 8986, 89861R (2014).

[12] S. Chuang and C. Chang, "k·p Method for Strained Wurtzite Semiconductors," Phys. Rev. B **54**, 2491–2504 (1996).

[13] S.-H. Park and S.-L. Chuang, "Crystal-orientation effects on the piezoelectric field and electronic properties of strained wurtzite semiconductors," Phys. Rev. B **59**, 4725–4737 (1999).

[14] R. G. Veprek, S. Steiger, and B. Witzigmann, "Reliable k·p band structure calculation for nanostructures using finite elements," J. Comput. Electron. **7**, 521–529 (2008).

[15] W. W. Chow, "Modeling of temperature and excitation dependences of efficiency in an InGaN light-emitting diode," Opt. Express **22**(2), 1413–1425 (2014).

[16] W. Scheibenzuber, U. Schwarz, R. Veprek, B. Witzigmann, and a. Hangleiter, "Calculation of optical eigenmodes and gain in semipolar and nonpolar InGaN/GaN laser diodes," Phys. Rev. B **80**, 115320 (2009).

[17] S. Brochen, J. Brault, S. Chenot, A. Dussaigne, M. Leroux, and B. Damilano, "Dependence of the Mg-related acceptor ionization energy with the acceptor concentration in p-type GaN layers grown by molecular beam epitaxy," Appl. Phys. Lett. **103**, 032102 (2013).

[18] T. Tanaka, A. Watanabe, H. Amano, Y. Kobayashi, I. Akasaki, S. Yamazaki, and M. Koike, "p-type conduction in Mg-doped GaN and Al0.08Ga0.92N grown by metalorganic vapor phase epitaxy," Appl. Phys. Lett. **65**, 593–594 (1994).

[19] J. Piprek, "AlGaN polarization doping effects on the efficiency of blue LEDs," Proc. SPIE 8262, 82620E (2012).

[20] G. Baraff, "Semiclassical description of electron transport in semiconductor quantum-well devices," Phys. Rev. B **55**, 10745 (1997).

[21] M. Deppner, F. Römer, and B. Witzigmann, "Auger recombination and carrier transport effects in III-nitride quantum well light emitting diodes," Proc. SPIE 8619, 86191J (2013).

[22] E. Kioupakis, Q. Yan, and C. G. Van de Walle, "Interplay of polarization fields and Auger recombination in the efficiency droop of nitride light-emitting diodes," Appl. Phys. Lett. **101**, 231107 (2012).

[23] B. Galler, P. Drechsel, R. Monnard, P. Rode, P. Stauss, S. Froehlich, W. Bergbauer, M. Binder, M. Sabathil, B. Hahn, and J. Wagner, "Influence of indium content and temperature on Auger-like recombination in InGaN quantum wells grown on (111) silicon substrates," Appl. Phys. Lett. **101**, 131111 (2012).

[24] C. Kölper, M. Sabathil, F. Römer, M. Mandl, M. Strassburg, and B. Witzigmann, "Core-shell InGaN nanorod light emitting diodes: Electronic and optical device properties," Phys. Status Solidi A **9**, 1–9 (2012).

[25] B. Galler, a. Laubsch, a. Wojcik, H. Lugauer, a. Gomez-Iglesias, M. Sabathil, and B. Hahn, "Investigation of the carrier distribution in InGaN-based multi-quantum-well structures," Phys. Status Solidi C **8**, 2372–2374 (2011).

[26] M. Grupen and K. Hess, "Simulation of carrier transport and nonlinearities in quantum-well laser diodes," IEEE J. Quantum Electron. **34**, 120–140 (1998).

[27] D. S. Meyaard, J. Cho, E. Fred Schubert, S.-H. Han, M.-H. Kim, and C. Sone, "Analysis of the temperature dependence of the forward voltage characteristics of GaInN light-emitting diodes," Appl. Phys. Lett. **103**, 121103 (2013).

1 Introduction

Solid state lighting based on blue InGaN/GaN light emitting diodes (LEDs) has become an enabling technology in the past years. The continued development of the device technology has led to a strong improvement of the crystal quality reducing defect related loss such as the Shockley-Read-Hall (SRH) recombination. Recent blue InGaN/GaN multi quantum well (MQW) LEDs show an internal quantum efficiency (IQE) of more than 80% [1]. The improvement of the doping profiles (particularly the acceptor doping) has contributed to the reduction of leakage related loss and the turn on voltage enhancing the wall plug efficiency (WPE). With the increase of the IQE another problem has become apparent, the efficiency droop [2]. When increasing the current density above 10 A/cm^2 a strong decay of the internal quantum efficiency can be observed. Since LED chip area is a key cost factor shifting the IQE maximum to higher current densities would contribute to a decrease of the overall costs for solid state lighting

devices. Identifying and quantifying the key droop mechanisms enables the development of strategies for reducing the effect of the droop in recent thin film LED structures.

In this context we propose the analysis of the IQE characteristics by physics based numerical simulation to complement the experiments. The work is targeted to the analysis of the contribution of the Auger recombination and direct carrier leakage to the droop by modeling the IQE. We demonstrate that the particularly the acceptor doping profile has a strong effect on the droop and that the effect of the Auger recombination increases with more than the third power of the carrier density.

For the origins of the droop Auger recombination, direct carrier leakage, and defect related processes have been proposed amongst others. The study presented in this work considers the Auger recombination and the direct carrier leakage as droop contributors. The direct carrier leakage is a major loss mechanism in some semiconductor lasers and also considered to be a major contributor to the droop in InGaN/GaN MQW LEDs [3]. Since the hole mobility in GaN is much lower than the electron mobility [4] the direct carrier leakage is mainly due to electron leakage.

Though Auger recombination and direct carrier leakage are different physical processes recent experiments and theoretical calculations have demonstrated that they indeed interact [5]. Considering the energy balance of the Auger process in the InGaN/GaN material system the particle receiving the energy is lifted from a quantum well (QW) state to the continuum. Due its high excess energy in the range of 2 eV the particle is prone to escape from the active zone more easily and contribute to the leakage current. Theoretical model calculations have shown that this Auger assisted leakage process can explain the droop with Auger coefficients reduced by a factor of up to two [5], and experimental evidence has been presented confirming the existence of the Auger assisted leakage process [6, 7]. Recent investigations on the phonon assisted Auger process show that the Auger recombination could be a major contributor to droop [8].

The model calculations are carried out with an advanced in-house developed semiconductor device physics simulator [9] which is described in section 2. Realistic figures of the Auger and direct carrier leakage contributions including the acceptor doping effect are obtained by numerically fitting experimental IQE data of InGaN/GaN single quantum well (SQW) and MQW LEDs emitting around 450 nm as presented in section 3. In section 4 we finally discuss the implications of the results and provide an outlook on the further development.

2 Physical Simulation

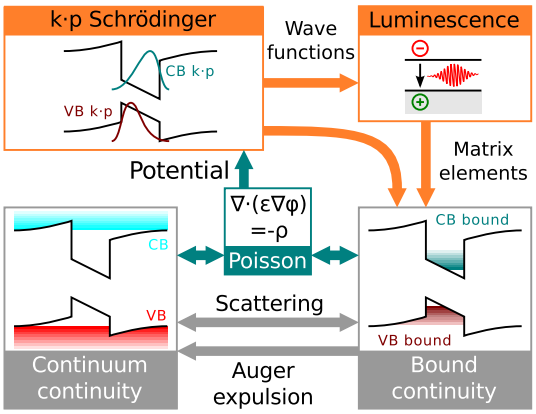

Figure 1: Operation scheme of the device simulation for an SQW LED.

The simulation model combines a drift/diffusion model for carrier transport and a multi band Schrödinger problem for the carrier quantization [10, 11]. Carriers divide into each one continuum electron and hole population and each one bound electron and hole population per quantum well (QW) as depicted in Fig. 1. The bound populations and the continuum population exist independently but are coupled by the mechanisms described in sections 2.1 and 2.2. The electron and hole distribution of each bound population is governed by a multi band $\mathbf{k} \cdot \mathbf{p}$ Schrödinger problem [12–14] in the direction of quantization. The computation of the wave functions extends beyond the limits of the QW region into the barriers. Particularly in the valence band bound states may be confined outside the QW region due to the strong piezoelectric polarization potential [15].

A microscopic luminescence model based on the transition matrix elements resulting from the $\mathbf{k} \cdot \mathbf{p}$ wave functions [16] provides the calculation of the radiative recombination. The luminescence model inherently accounts for phase space filling and screening [10]. The interpretation of the results is supported by an effective radiative coefficient B_{eff} extracted for each QW. This effective radiative coefficient relates the integral electron and hole densities to the total radiative recombination of the quantum well so that it directly compares to the B-coefficient entering an ABC-model [3]:

$$B_{\mathrm{eff}} = d_{\mathrm{QW}} \frac{R^q_{\mathrm{rad}}}{n_q p_q - n^2_{\mathrm{i,q}}}. \tag{1}$$

The values n_q and p_q are the two dimensional electron and hole density and $n_{\mathrm{i,q}}$ is the intrinsic density in the QW. The effect of the overlap integral is implicitly included in the radiative recombination rate R^q_{rad} due to the microscopic luminescence model. The coefficient is weighted with the effective quantum well width d_{QW} to render a volume unit.

An incomplete activation model based on the Shockley defect recombination model determines the donor and acceptor ionization and thus the active doping charge. The acceptor ionization energy of GaN has been set to $E_A(N_A \rightarrow$

0) = 245 meV and depends on the doping density [17]. It can be expected that the acceptor ionization energy of $Al_{0.1}Ga_{0.9}N$ is about $\approx kT$ higher [18]. Considering the uncertainty of the doping density and the acceptor ionization energy as reported in [17] the acceptor ionization energy $E_A(N_A \to 0) = 245$ meV has been also applied to the AlGaN alloy. The Poole-Frenkel effect [19] has not been included.

2.1 Dynamic scattering

The transport of carriers to and from the quantum wells is governed by the energy space instead of the real space using a dynamic scattering mechanism [20]. The dynamic scattering model is a phenomenological approach to the phonon emission and absorption processes. It is controlled by the difference of the quasi Fermi levels and therefore conforms to the thermal equilibrium conditions. A net carrier transition from continuum to bound as well as from bound to continuum population may occur. Thus, thermionic emission processes are included implicitly in the model. The scattering rate is controlled by the phenomenological scattering time parameter τ_{sc}. The net local scattering decay rate for the continuum electrons is therefore

$$R_{\mathrm{sc,e}} = \frac{n}{\tau_{\mathrm{sc}}} \left(1 - \exp\left(\frac{E_{\mathrm{F,q}} - E_F}{k_B T}\right)\right) \left(1 - \frac{n_q}{N_q}\right) \sigma_{\mathrm{sc}}(x_q). \tag{2}$$

Here, n is the local continuum electron density and N_q the 2D density of electron states in the QW. E_F and $E_{\mathrm{F,q}}$ are the Fermi energies in the continuum and the QW, respectively. The function $\sigma_{\mathrm{sc}}(x_q)$ is a unit-less scattering distribution function in the direction of the quantization. A similar relation is used for the hole scattering.

For interpreting the results an effective scattering time τ_{eff} is extracted. The effective scattering time is the actual lifetime of the transition of continuum carriers to the QW and evaluates to

$$\tau_{\mathrm{eff}} = \frac{\int n \sigma_{\mathrm{sc}} \, \mathrm{d}x_q}{\int R_{\mathrm{sc}} \, \mathrm{d}x_q}. \tag{3}$$

where the integration runs over the direction of quantization x_q.

2.2 Auger expulsion

The second mechanism contributing to the coupling of bound and continuum carriers is the Auger recombination in the bound populations. The simulator implements an advanced Auger recombination model [21] for bound populations which includes the overlap integral of the electron and hole wave functions [22]. The electron as well as the hole Auger recombination are controlled by the parameters C_n and C_p, respectively so that

$$\begin{aligned} R^q_{\mathrm{Aug,e}} &= C_n n_q (n_q p_q - n^2_{\mathrm{i,q}}) \int \psi^2_{\mathrm{e}} \psi_{\mathrm{h}} \, \mathrm{d}x_q \\ R^q_{\mathrm{Aug,h}} &= C_p p_q (n_q p_q - n^2_{\mathrm{i,q}}) \int \psi^2_{\mathrm{h}} \psi_{\mathrm{e}} \, \mathrm{d}x_q \end{aligned} \tag{4}$$

where ψ_{e} and ψ_{h} are the electron and hole envelope wave functions. The integral applies for the quantized direction x_q. The coefficients C_n and C_p enter the

simulation model as parameters and have the unit and denotation of bulk Auger coefficients. Since the envelope wave functions enter the Auger model it is subject to screening, just as the radiative recombination. Similar to the effective radiative coefficient B_{eff} an effective Auger coefficient C_{eff} for the total Auger recombination of each QW is extracted that compares to the C coefficient of an ABC-Model:

$$C_{\mathrm{eff}} = d_{\mathrm{QW}}^2 \frac{R_{\mathrm{Aug,e}}^q}{n_q(n_q p_q - n_{\mathrm{i,q}}^2)} + d_{\mathrm{QW}}^2 \frac{R_{\mathrm{Aug,h}}^q}{p_q(n_q p_q - n_{\mathrm{i,q}}^2)}. \tag{5}$$

The actual electron and hole drain rate is due to the Auger recombination and the expulsion process because the electron or hole receiving the energy of the recombination is also removed from the QW population. This particle is added to the continuum population where the real space position is subject to the bound wave function. Thus, the electron Auger process removes twice as much electrons as holes and the hole Auger process removes twice as much holes as electrons from the QW population. The Auger leakage effect has been neglected for the IQE model calculations so that all particles expelled from a QW enter the continuum population.

3 Droop analysis

For the assessment of the effect of Auger recombination and direct carrier leakage on droop the experimental IQE data of an InGaN/GaN SQW as well as an MQW LED with blue emission around 450 nm have been analyzed [23,24]. The SQW LED has been subject to a more detailed analysis because the extracted parameters B_{eff}, C_{eff}, and τ_{eff} apply for the whole device which is not given for the MQW LED. Hence, the interpretation of these parameters is easier and more straight forward for an SQW LED.

It is commonly understood that from a pure physical point of view the effect of the Auger recombination can be reduced by increasing the active volume with the number of QWs. Thus, the average carrier density can be reduced and the dominance of the Auger recombination as compared to the radiative recombination reduces. This means that MQW LEDs are less affected by the Auger recombination than SQW LEDs. On the other hand side, the effect of the direct carrier leakage is hard to predict because it depends on many geometric and material related factors, including the doping profile and the design of the electron blocking layer (EBL). Moreover, since injection usually results in an unequal distribution of the luminescence amongst different QWs in an MQW device [25] it has also some effect on the Auger recombination.

3.1 Single quantum well LED

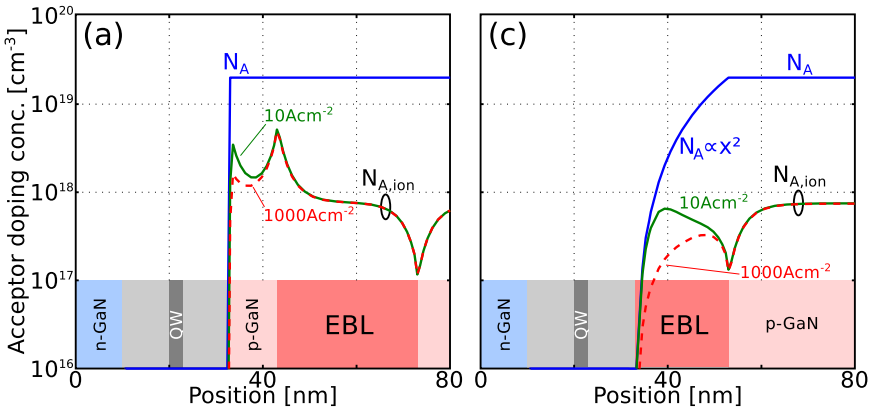

Figure 2: Left: SQW LED design (a) with abrupt doping profile and p-doped spacer layer between EBL and barrier. Right: SQW LED design (c) with graded doping in the EBL. The acceptor doping density N_A and the ionized acceptor density $N_{\mathrm{A,ion}}$ are shown for 10 Acm^{-2} (solid) and 1000 Acm^{-2} (dashed). The ionized acceptor density decreases with increasing hole injection.

The IQE of the SQW LED presented in [23] has been used for studying the effect of Auger recombination and leakage. The IQE has been intentionally fitted for different designs with varying Auger coefficients to investigate the sensitivity of the IQE to structural and simulation parameters and to estimate the significance of Auger recombination and direct carrier leakage for the droop. The different structures are shown in Fig. 2. The top structure in Fig. 2 is an abrupt acceptor doping profile design that is the primary target of investigation. This design is expected to show low direct carrier leakage so that the limits of the Auger coefficients may be estimated. The active zone consists of one 3 nm wide $In_{0.19}Ga_{0.81}N$ QW embedded in two 10 nm wide barriers. The weak p-doping ($N_A = 10^{16}\mathrm{cm}^{-3}$) of the active zone has virtually no effect on the IQE characteristics. The 30 nm wide $Al_{0.1}Ga_{0.9}N$ EBL is separated by a 10 nm wide p doped GaN spacer layer from the active zone. The Auger coefficients C_n and C_p, the electron scattering parameter $\tau_{sc,e}$, and the SRH life time τ_{SRH} have been varied to match the simulated IQE characteristics. Auger expulsion has been enabled. All expelled carriers are added to the continuum population. The doping concentrations are $N_A = 2 \times 10^{19}\mathrm{cm}^{-3}$ in the p-zone including the spacer layer and the EBL and $N_D = 6 \times 10^{17}\mathrm{cm}^{-3}$ in the n-zone. The density of ionized acceptors is far lower than the acceptor doping density because of the high acceptor activation energy as illustrated in Fig. 2. The ionized acceptor density decreases with rising current in the vicinity of the active zone because the higher injection of holes decreases the acceptor ionization.

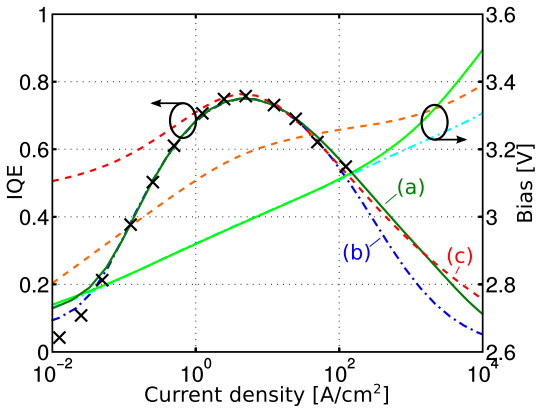

Figure 3: Measured IQE data (crosses) from [23] versus IQE simulation for the SQW design with EBL (a) (solid), without EBL (b) (dash dot), and with graded doping in the EBL (c) (dashed).

Table 1: Model parameters of the SQW LED simulations.

	$C_{\mathrm{n/p}}$, [cm^6/s]	τ_{SRH} [s]	B_{min} [cm^3/s]	C_{min} [cm^6/s]
(a)	4.0×10^{-31}	1.40×10^{-7}	4.79×10^{-12}	2.17×10^{-31}
(b)	3.7×10^{-31}	1.35×10^{-7}	4.72×10^{-12}	1.98×10^{-31}
(c)	0	0.90×10^{-7}		0

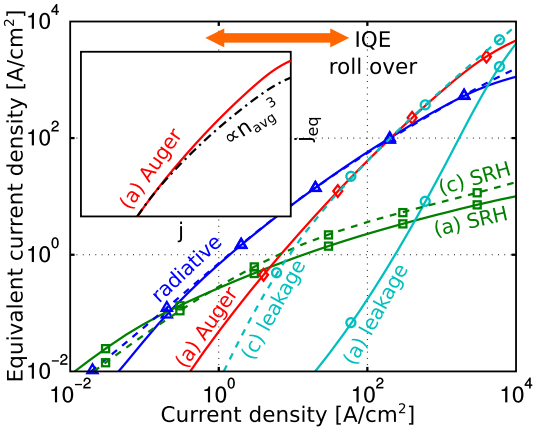

Figure 4: Equivalent current contributions to SRH, radiative, and Auger recombination as well as direct carrier leakage versus the total current. Curves (a) hold for the abrupt doping profile design. Curves (c) are for the graded doping profile. The inset depicts the Auger recombination versus the third power of $n_{\mathrm{q,avg}} = (n_q + p_q)/2$ in the QW.

The simulated IQE curve is shown together with the experimental data in Fig. 3. Curve (a) shows the simulated IQE for the abrupt doping profile as

shown in Fig. 2(a). In order to examine the sensitivity of the Auger coefficients the IQE has been also simulated for this structure without EBL which is the design (b). For this design the Auger coefficients have been reduced so that the related IQE curve does not show a significant deviation from (a) when comparing it to the measured data. The coefficients entering the model are collected in Table 1. The electron scattering parameter is $\tau_{\mathrm{sc,e}} = 7 \times 10^{-12}$s for all simulations. This value has been obtained matching the IQE characteristics as well as the luminescence distribution amongst the quantum wells of the MQW structure and is in good agreement with reported and experimentally verified values [26].

It is noted that the Auger parameters required for matching the design (b) are less than 10% lower than the coefficients of design (a) suggesting that even without an EBL the direct carrier leakage has only a minor impact in the IQE roll over zone if the acceptor doping is sufficiently high close to the active region. This observation has been verified by analyzing the contributions of the different loss mechanisms to the IQE as shown in Fig. 4. The radiative recombination is clearly dominating in the roll over zone, but the most dominant loss mechanism is the Auger recombination. The contribution of the direct carrier leakage is about two orders of magnitude lower than the contribution of the Auger recombination to the loss. Thus, the Auger coefficients extracted for the design (a) establish an upper limit. Recent quantum mechanical simulations of the active region of an InGaN/GaN SQW LED explain the droop with similar Auger coefficient values [15].

Figure 4 demonstrates that the droop edge is determined by the gradient of the dominating loss mechanism with respect to the current density. Since the gradient of the direct carrier leakage is higher than the gradient of the Auger recombination it is not sufficient to increase direct carrier leakage and decrease the Auger recombination for fitting the IQE. However, the graded doping profile structure depicted in Fig. 2 affects the direct carrier leakage so that its gradient matches the gradient of the Auger recombination as shown in Fig. 4. Consequently, the IQE characteristics may be explained without Auger recombination at all for a specific doping profile.

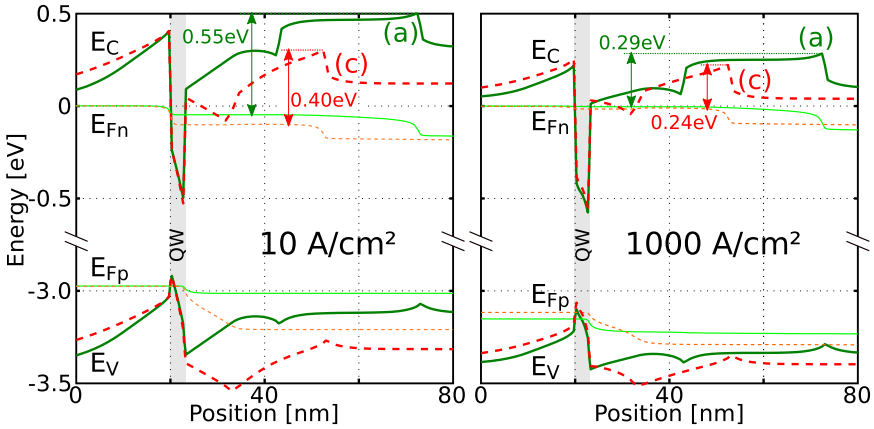

Figure 5: Band structure and quasi Fermi levels of the design (a) with abrupt doping profile and the design (c) with graded doping at 10 Acm^{-2} and 1000 Acm^{-2}. The barrier height difference between (a) and (c) reduces with rising current.

Comparing the band structures of both designs shown in Fig. 5 for a current density of 10 Acm^{-2} and 1000 Acm^{-2} provides an explanation for the change of the leakage characteristics. The electrons passing the QW observe a lower energy barrier to the p-region in the graded doping design. This barrier reduction is due to the positive polarization charge at the left interface of the EBL. In the abrupt doping profile structure this sheet charge is nearly screened by the negative charge of the ionized acceptors. In the graded doping profile structure the acceptor doping is not high enough to screen the sheet charge, so that the barrier for electrons is lowered. When increasing the current more holes are injected so that the screening improves. Increasing the current reduces the electron barrier height for both the structure with abrupt and graded doping profile, but the decrease of the barrier height is lower for the graded doping profile (0.16 eV) than for the abrupt doping profile (0.26 eV). To the end, the different decrease of the barrier height explains the different gradient of the leakage characteristics observed in the structures (a) and (c).

It shall be pointed out that the intention of different designs is to demonstrate the ambiguity of the IQE with respect to the structural parameters. The central statement is that the IQE is very sensitive to the acceptor doping profile, particularly in combination with an EBL. A highly p-doped EBL can suppress leakage while an insufficient p-doping combined with an EBL reduces the barrier for electron leakage. When analyzing the IQE characteristics with lumped models, particularly the ABC model, it is obvious that designs (a) and (c) render nearly the same loss coefficients. The physics based simulations demonstrate that even for an SQW LED it is not possible to attribute any of the fitted loss coefficients to a particular loss mechanism.

The significant difference in the current versus voltage characteristics of the designs (a) and (c) suggests that this property could be used to resolve the ambiguity and to obtain more reliable figures of the Auger recombination and direct carrier leakage effect. According to Fig. 3 the forward voltage is about 3.0 V at maximum IQE for the abrupt doping profile and about 3.2 V for the

graded doping profile. The lower value is closer to experimental data [27] of recent InGaN/GaN LEDs.

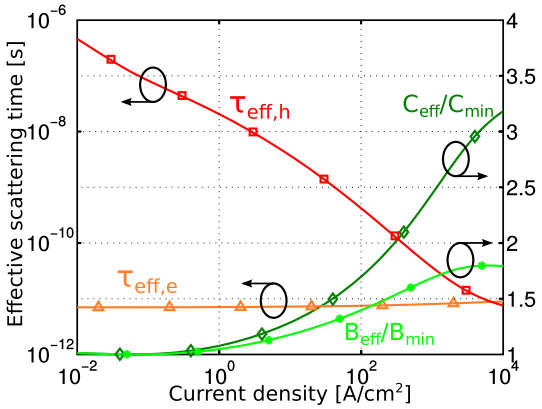

Figure 6: Effective scattering time for electrons (triangles) and holes (squares) and relative effective radiative (stars) and Auger coefficient (diamonds) for the design with abrupt doping profile and EBL.

For the structure with the abrupt doping profile the effective scattering time and the effective radiative and Auger coefficients have been analyzed. Notably, the effective electron scattering time $\tau_{\mathrm{eff,e}}$ remains at its lower limit over the full current range whereas $\tau_{\mathrm{eff,h}}$ decreases for rising current according to Fig. 6. The electron capture is limited by the scattering time parameter because the high conduction band offset effectively separates the quasi Fermi level in the continuum and the quantum well. Decreasing the electron scattering time increases the net electron transition rate to the QW, but this has only a minor effect on the IQE because the leakage contribution is already low in the IQE roll over zone. The hole capture is less affected by $\tau_{\mathrm{eff,h}}$ because the quasi Fermi levels of continuum holes are quite close to the valence band edge in the QW as depicted in Fig. 5. The proximity of the Fermi levels is partly due to the lower valence band offset and the Fermi levels are less sensitive to variations of the carrier density because of the higher valence band density of states. Therefore, the hole scattering time parameter has little influence of the simulation results.

The increase of the effective Auger and radiative coefficients with rising current depicted in Fig. 6 can be attributed to the screening of the polarization charge by carrier injection into the QW. The increase of the radiative coefficient is weaker which may be attributed to the phase space filling. However, it is even weaker at low currents where the phase space filling effect is negligible. Thus, the screening effect on the Auger recombination is also stronger due the difference in the overlap integrals entering the Auger recombination model Eq. (5) and the luminescence model.

As illustrated in the inset of Fig. 4 the increase of the Auger recombination is higher than the third power of the carrier density due to the effect of the overlap integral. Considering a lumped IQE model, the Auger recombination contributes also to $O(n^4)$ and higher order terms also in the view of the radiative recombination. Thus, the higher order coefficients may be at least partially due to the Auger process instead of direct carrier leakage.

3.2 Multi quantum well LED

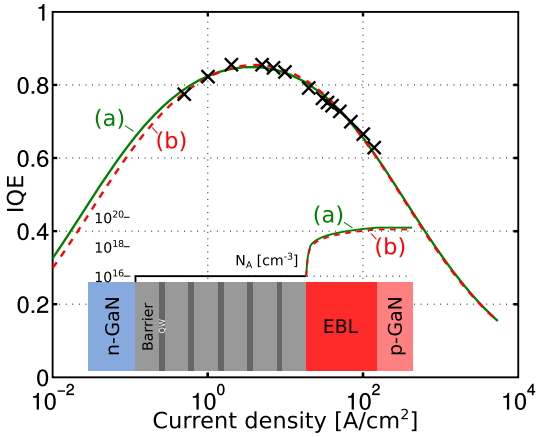

Figure 7: Measured IQE data (crosses) from [24] versus IQE simulation for different graded doping in the EBL. The maximum doping density is $N_A = 2 \times 10^{19}$ cm^{-3} for (a) (solid) and $N_A = 1.5 \times 10^{19}$ cm^{-3} for (b) (dashed)

Table 2: Model parameters of the MQW LED simulations.

	$N_{\mathrm{A},0}$[cm^{-3}]	$C_{\mathrm{n/p}}$, [cm^6/s]	τ_{SRH} [s]
(a)	2×10^{19}	4.0×10^{-31}	5.0×10^{-7}
(b)	1.5×10^{19}	2.8×10^{-31}	4.5×10^{-7}

The IQE has been simulated for a MQW LED with 5 QWs emitting at 440 nm as presented in [24]. The active zone consists of five 3 nm wide $In_{0.17}Ga_{0.83}N$ QW separated by 10nm wide GaN barriers and is slightly p-doped ($N_A = 10^{16}$cm^{-3}). A 30 nm wide $Al_{0.15}Ga_{0.85}N$ EBL terminates the active zone on the p side. The donor doping is $N_D = 8 \times 10^{17}$cm^{-3}. For matching the measured IQE data the acceptor doping, the SRH lifetime, and the Auger coefficients have been varied amongst others. Auger expulsion has been enabled. The electron scattering time was found to be identical to the one of the SQW LED ($\tau_{\mathrm{sc,e}} = 7 \times 10^{-12}$s). The measured IQE characteristics cannot be explained by the Auger recombination alone. In order to match the droop a graded acceptor doping in the EBL has been assumed. The acceptor doping in the EBL varies linearly from the active zone doping to $N_{\mathrm{A},0}$ in the quasi neutral p-region. For the simulations shown in Fig. 7 the value $N_{\mathrm{A},0}$ and the Auger parameter have been varied as listed in Table 2. Both simulations agree with the measured data in a similar way.

It is noted that the Auger coefficients are lower than for the SQW LED which may be attributed to the Auger leakage [5] effect. It can be expected that the Auger leakage in the MQW LED is not as pronounced as in the SQW LED because of the larger extent of the active region so that fitted Auger coefficients would be typically smaller. The implication of the Auger leakage is that the IQE of the SQW LED design (a) may be explained with Auger coefficients as

low as $C_{\mathrm{n/p}} = 2.0 \times 10^{-31}$ cm^6/s which are in the range of the bulk coefficients predicted by atomistic simulations [8].

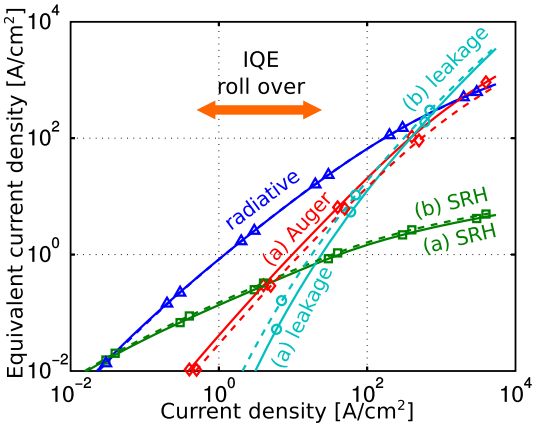

Figure 8: Equivalent current contributions to SRH, radiative, and Auger recombination as well as direct carrier leakage versus the total current for the MQW LED and for the doping profiles (a) and (b).

The multiple QWs present an effectively higher active volume so that the Auger recombination is less dominant than in the SQW LED. The direct carrier leakage depends much on the acceptor doping profile so that it can vary over a large range. Figure 8 illustrates that in the roll over zone of IQE the contribution of the leakage is higher than in the SQW LED design (a) though the Auger recombination still dominates. Therefore a variation of the design parameters affecting the leakage are seen through a change of the Auger parameters. The variation of the simulation parameters is in a physically and technically permitted range, so that it is not possible to discard a solution. This confirms the ambiguity of the simulation parameters which has been pointed out in the introduction of this section.

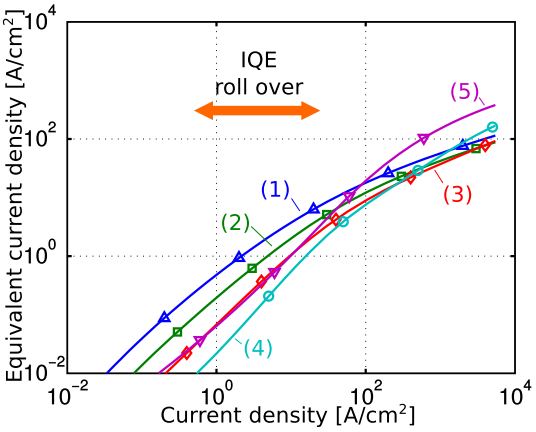

Figure 9: Luminescence contribution of each QW for the MQW LED with doping profile (a). The quantum well (1) is next to the n-region. The quantum well (5) is next to the EBL.

The luminescence contribution of the QWs is depicted in Fig. 9 for the design (a). The figures for the design (b) do not differ significantly and have therefore been omitted for clarity. The results shown here conform to the observation that the QW next to the p-region starts to dominate the luminescence at LED operation currents above $j = 50$ Acm^{-2} [25]. The low hole mobility of about 5 cm^2/Vs limits the hole spreading so that the n-side QWs are not sufficiently supplied with holes at high currents. It is noted that the luminescence distribution is also sensitive to the electron scattering time. As pointed out in section 3.1, the electron capture is hardly affected by the quasi Fermi levels, so that the distribution of electrons amongst the QWs is affected by the scattering time parameter. Increasing the electron scattering time enhances the luminescence of the p-side QW but also increases the leakage because of the reduced capture efficiency. Decreasing the electron scattering time parameters enhances the luminescence contribution of the n-side quantum well and reduces leakage. In the roll over zone the effect on the IQE is small, though, because the direct carrier leakage contribution is lower than the Auger recombination.

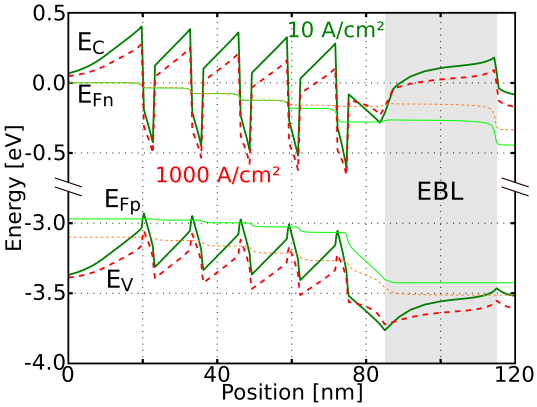

Figure 10: Band structure and quasi Fermi levels of the MQW LED (a) at 10 Acm^{-2} (solid) and 1000 Acm^{-2} (dashed).

The different scattering of electrons and holes reflects in the continuum quasi Fermi levels depicted in Fig. 10. The continuum quasi Fermi level of the holes is merely fixed with respect to the band edge for different currents. The electron quasi Fermi level is not fixed. At high currents the electrons increasingly escape from the active region because the electron scattering is limited. The electron overflow increase with the current is seen through a strong increase of the continuum quasi Fermi levels for the electrons in the QWs close to the p-doped region.

4 Conclusion

We have demonstrated the physics based simulation of InGaN/GaN SQW and MQW LEDs emitting around 450 nm. The simulation method is based on the device structure and separates the transport problem in bound and continuum populations coupled by scattering mechanisms and a global electrostatic potential. The crucial parameters controlling the scattering and the Auger recombination have been found to be identical for different devices when fitting measured IQE curves and are in the range predicted by quantum transport or atomistic models confirming the significance of our simulation approach.

The investigation of the SQW LED revealed that particularly the p-doping profile has a major impact on the droop. However, with a realistic doping profile the Auger recombination provides a consistent explanation for the droop and is the dominating loss mechanism in the roll over zone of the IQE. Fitted Auger coefficients of the SQW and the MQW LED are quite similar while the difference my be explained by the effect of the Auger leakage. Due to polarization charge screening the Auger recombination may increase stronger than with the third power of the carrier density leading to higher order terms in a lumped IQE model.

The strong effect of the doping profile demonstrates that even for an SQW LED the simulation of the IQE cannot be reduced to the simulation of the QW only. The significance of the Auger coefficient extraction might be enhanced by including the current versus bias voltage (I/V) characteristics which is sensitive

to the p-doping profile so that a more reliable estimate of the direct carrier leakage may be extracted. In an outlook, a tunneling model for the piezo potential barriers would enable a more precise simulation of the I/V characteristics. A better model for the Auger expulsion and the Auger leakage process could be achieved by a hydrodynamic simulation approach where the carrier populations need not be in thermal equilibrium with the lattice.